

Charge Transfer Absorption and Emission at ZnO/Organic Interfaces

Fortunato Piersimoni,^{*,†} Raphael Schlesinger,[‡] Johannes Benduhn,[§] Donato Spoltore,[§] Sina Reiter,[†] Ilja Lange,[†] Norbert Koch,[‡] Koen Vandewal,^{*,§} and Dieter Neher^{*,†}

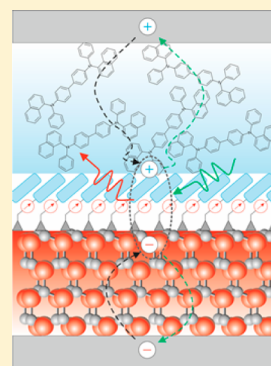
[†]Institute of Physics and Astronomy, University of Potsdam, Karl-Liebknecht-Straße 24-25, 14476 Potsdam, Germany

[‡]Institut für Physik & IRIS, Adlershof Humboldt-Universität zu Berlin, Brook-Taylor-Straße 6, 12489 Berlin, Germany

[§]Institut für Angewandte Photophysik, Technische Universität Dresden, George-Bähr-Straße 1, 01069 Dresden, Germany

S Supporting Information

ABSTRACT: We investigate hybrid charge transfer states (HCTS) at the planar interface between α -NPD and ZnO by spectrally resolved electroluminescence (EL) and external quantum efficiency (EQE) measurements. Radiative decay of HCTSs is proven by distinct emission peaks in the EL spectra of such bilayer devices in the NIR at energies well below the bulk α -NPD or ZnO emission. The EQE spectra display low energy contributions clearly red-shifted with respect to the α -NPD photocurrent and partially overlapping with the EL emission. Tuning of the energy gap between the ZnO conduction band and α -NPD HOMO level (E_{int}) was achieved by modifying the ZnO surface with self-assembled monolayers based on phosphonic acids. We find a linear dependence of the peak position of the NIR EL on E_{int} , which unambiguously attributes the origin of this emission to radiative recombination between an electron on the ZnO and a hole on α -NPD. In accordance with this interpretation, we find a strictly linear relation between the open-circuit voltage and the energy of the charge state for such hybrid organic–inorganic interfaces.



There is a great interest in the scientific community toward organic electronics, mainly drawn from the perspective of novel optoelectronic applications. Because of their low dielectric constant, optical absorption in organic materials leads to the formation of Frenkel-type excitons, spatially localized electron–hole pairs with a binding energy in the range of half an electronvolt. The need to overcome such binding energies requires the use of type II heterojunctions comprising an electron donor (D) and an electron acceptor (A) material, where the difference in frontier energy levels results in a driving force for exciton dissociation.

Up to now, the highest exciton dissociation efficiencies were obtained by using organic semiconductors (OSCs) as both the donor and the acceptor. It is widely accepted that the photoinduced electron transfer from the donor to the acceptor does not necessarily result in fully separated charges but rather in the formation of an intermediate charge transfer state (CTS).^{1–7} Different theories regarding the role of such CT states in the process of free charge generation and recombination have been put forward, and experimental results are still contradictory.^{3,8,9} However, the interpretation and comparison of these findings is aggravated by the fact that the organic/organic heterojunction is morphologically and electronically rather ill-defined. This is particularly true for bulk heterojunction devices, where intermixing of the components at the local donor–acceptor interface or even on the more mesoscopic scale has been proven for many systems.

Hybrid devices comprising an inorganic and organic semiconductor offer an exciting alternative to all organic solar cells. In particular, metal oxides provide a wide chemical variability combined with high electron or hole mobilities.

Some of these oxides can be deposited with different vapor- or solution-based techniques, offering various methods to structure the material and thereby its interface to the organic partner. Fine tuning of the surface energetics via physisorption or chemisorption of suitable molecules has been demonstrated for a wide range of materials. Finally, given the fact that most metal oxides are not soluble in common organic solvents, the preparation of chemically and structurally well-defined heterojunctions is quite straightforward. Despite these possibilities, only few publications, however, deal with the electronic structure, formation, and dissociation of CT states at hybrid organic–inorganic interfaces.^{10–15}

Haeldermans et al. were able to resolve a subgap signal in the external quantum efficiency (EQE) spectrum of TiO₂:P3HT solar cell and related this to the direct excitation of a hybrid charge transfer state (HCTS).¹⁰ More recently an extra feature in the electroluminescence (EL) spectra of CdS:P3HT device, not present in the pure materials, was detected and associated with HCTS emission.¹¹ Some evidence of the existence of HCTSs at the ZnO/organic interface comes from steady-state photoluminescence (PL) studies on ZnO nanorod/P3HT heterojunctions, although the emission from these hybrid excitations was largely obscured by the stronger PL from P3HT.¹⁶ Femtosecond optical pump–push photocurrent measurements performed by Vaynzof et al.¹⁴ suggested that electron–hole pairs formed at the ZnO/organic interface are strongly bound. In agreement to this, recent theoretical work

Received: December 17, 2014

Accepted: January 15, 2015

Published: January 15, 2015



on the energetics and dynamics of excitations at the ZnO/P3HT interface stated that the presence of defects at the ZnO surface gives rise to highly localized (perpendicular and parallel to the interface) and electrostatically bound HCTSs.¹⁵ Theoretical and experimental work by Forrest and coworkers, on the other hand, suggested efficient charge generation across the hybrid interface due to a low binding energy of the hybrid charge transfer states.^{12,13}

A charge-transfer state is, per definition,¹⁵ “a state related to the ground state by a charge transition”.¹⁷ This implies that the charge-transfer state CTS can radiatively recombine to, or be optically excited from, the ground state. Indeed for various organic donor–acceptor systems, radiative CTS decay has been reported. Also, absorption of low-energy light via direct CTS excitation has been observed for many organic–organic systems.^{2,4,18}

In the present work we detect the emission and the absorption from HCTS at the planar interface between an inorganic electron acceptor, ZnO and organic donor, *N,N'*-di(1-naphthyl)-*N,N'*-diphenyl-(1,1'-biphenyl)-4,4'-diamine (α -NPD). We show the ability to vary the energy of the CT state by tuning the work function of the ZnO layer with self-assembled monolayers and observe a corresponding shift in the CT emission spectra. This shift is shown to correlate with the open-circuit voltage (V_{oc}) of hybrid α -NPD/ZnO photovoltaic devices and the energy gap between the HOMO of the donor and the conduction band (CB) of the acceptor, as measured by photoelectron spectroscopy.

For this study on hybrid CT states, we choose α -NPD in combination with ZnO for several reasons. First, with α -NPD HOMO level energy at ca. 5.5 eV and the ZnO CB minimum at ca. 4 eV, the energy gap at the hybrid interface is expected to be at ~ 1.5 eV, and CT emission as well as CT absorption (or EQE) spectra should be accessible with established equipment. Also, with an energy gap of almost 3 eV, absorption and emission from the α -NPD bulk is expected to be spectrally well-separated from any optical feature related to the HCTS. The same is true for ZnO, which is transparent above ca. 3.3 eV and has an only weak emission in the visible wavelength range.

We employed microcrystalline sol–gel-processed ZnO,¹⁹ for which by AFM we observed the crystallites to have sizes within 10 nm, leading to an RMS surface roughness around 2 nm. Because the most stable surfaces of ZnO are the (0001), (000 $\bar{1}$), and (10 $\bar{1}$ 0) facets, we expect the sol–gel ZnO surface to consist mainly of these three facets. It was observed in the literature that the shift in work function upon phenylphosphonate treatment does not depend on the crystal orientation and the morphology of the ZnO layer.²⁰

The inset of Figure 1 shows the PL and optical absorption spectrum of a layer of pure α -NPD together with EL of an α -NPD deposited on ZnO containing device, plotted on a linear scale. The spectra of pure α -NPD show only bulk emission and absorption with no evidence of subgap states. Contrarily, the EL spectrum of α -NPD deposited on ZnO reveals complete quenching of the bulk emission, while a broad peak centered on 1.1 eV appears. We, therefore, assign this emission to the radiative decay of HCTSs. To confirm this assignment, EQE spectra were measured over a wide range in energy and sensitivity. (See Figure 1.) The EQE spectrum shows a maximum, related to the α -NPD absorption, at ~ 3.2 eV, but the spectrum extends far below the energy gap of α -NPD, down to 1.3 eV. The spectral overlap of this low-energy tail of the EQE with the high-energy side of the EL peak and also the

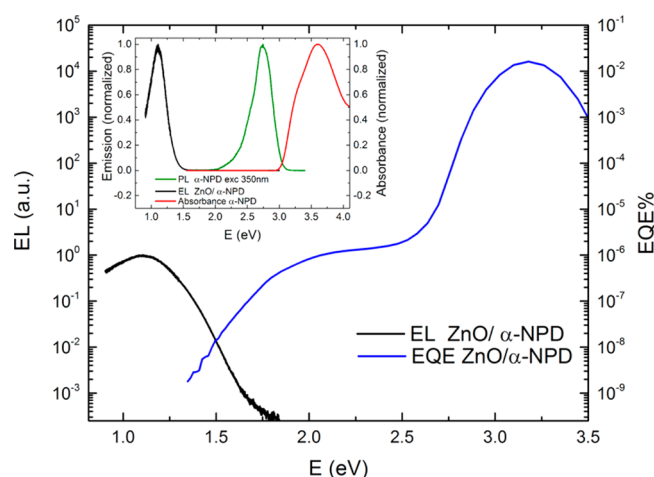


Figure 1. Electroluminescence intensity (EL) and external quantum efficiency (EQE) for a planar bilayer device using α -NPD as the donor and ZnO as the acceptor (logarithmic scale). The inset shows the PL and absorption from a neat α -NPD thin film and EL of α -NPD deposited on ZnO (linear scale).

similar spectral width of these two features suggests that both originate from the same state,²¹ centered at ca. 1.5 eV. Notably, compared with most all-organic donor–acceptor systems, the Stokes shift between CT emission and absorption is rather high, ~ 0.9 eV (Figure S2 in the Supporting Information). This indicates either a large relaxation energy or, alternatively, inhomogeneous broadening due to tail states.²¹

As previously pointed out, precedent works assigned subgap signal in the EL¹¹ or EQE¹⁰ spectra from hybrid bulk heterojunctions to the emission, respectively, absorption of HCTSs. To the best of our knowledge, our case is the first time that both emission and absorption are detected from a hybrid planar interface in a spectral region where the HCTS is expected.

The possibility to tune the work function of a ZnO layer is an important tool to control the properties of hybrid interfaces. A known method to achieve this is the formation of a self-assembled monolayer with molecules carrying appropriate dipole moment onto the ZnO surface.^{22–24} We have recently developed a preparation protocol, which leads to a very dense and homogeneous monolayer of oriented molecules on ZnO substrates, without etching effects.²⁵ By employing substituted benzylphosphonic acids (BPAs) as well as pyrimidin phosphonic acid (PyPA) with different dipole moments of the headgroup, Lange et al. succeeded to alter the workfunction (measured with Kelvin Probe) from about 4.1 eV to almost 5.7 eV.²⁵

Here we employ a variety of substituted BPAs, in particular, 4-aminobenzylphosphonic acid (ABPA), BPA, and blends in different ratios of BPA with 4-bromobenzylphosphonic acid (Br-BPA) on sol–gel-processed ZnO to tune the ZnO's effective work function and thus the α -NPD HOMO position relative to the ZnO energy levels. Photoelectro spectroscopy (PES) was employed to determine the energy levels of ZnO and α -NPD. (See Figure S3 in the Supporting Information.) The ZnO Zn 2p core-level shift upon SAM and α -NPD deposition was used to correct the ZnO energy levels for internal band bending induced by the chemisorption of the SAM.²⁶ The CB minimum position of bare ZnO is considered to be 0.1 eV above the Fermi level.

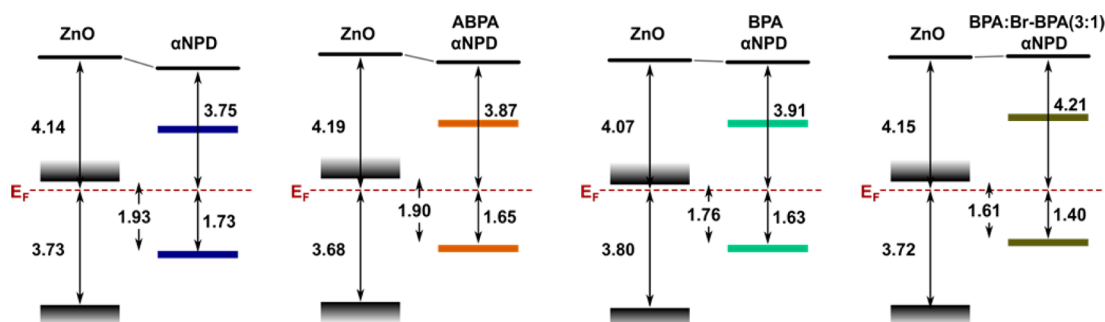


Figure 2. Energy levels of α -NPD at the interface with different SAMs grown on ZnO. By employing different SAM interlayers the gap between the α -NPD HOMO and the ZnO conduction band minimum is successively reduced. The corresponding photoemission data are shown in Figure S3 in the Supporting Information. The ZnO energy level positions were corrected for the adsorption induced internal band bending.

The resulting gaps between the CB minimum of ZnO and the HOMO onset of α -NPD at the hybrid heterojunction are plotted in Figure 2 and firmly prove that increasing the ZnO work function leads to a continuous decrease in the energy gap from 1.9 to 1.6 eV. This is accompanied by a corresponding red shift of the maximum of the EL spectra, as shown in Figure 3. The spectral position of the EL maximum is plotted in the inset of Figure 3 as a function of the D/A energy gap. The linear dependence of the emission energy versus the energy gap rules out that the EL originates from defect states in the bulk of the two materials or at the interface. It provides a clear indication that this emission originates from the radiative recombination of electrons in the acceptor with holes in the donor, located at the hybrid interface.

The same samples were then used to measure EQE spectra. Unfortunately the low-energy tail assigned to a transition from the ground state to the HCTS was largely suppressed in these layers, probably due the presence of a SAM between donor and acceptor, which increases their distance and reduces the oscillator strength of the transition. (See Figure S1 in the Supporting Information.) Therefore, the sensitivity of the current setup did not allow us to clearly detect the onset of the photocurrent. This will be the subject of future work.

Recent experiments on all-organic donor–acceptor solar cells established a linear correlation between the energy of the CTS

and the V_{oc} of the device.²⁷ Figure 4 shows the J – V characteristics of several planar hybrid devices, with the ZnO work function now varied over a larger range by employing pure Br-BPA as well as a 1:1 mixture with BPA. The J – V curves in Figure 4 display a large and continuous reduction of the V_{oc} from 0.96 V down to ca. 0.2 V, with increasing ZnO work function. The plot of V_{oc} as a function of the EL emission maximum (see the inset of Figure 4) reveals a linear dependence, pointing to a similar correlation between CT energy and V_{oc} as reported for all-organic type-II heterojunction devices.

The reproducibility of the results is mostly related to factors that may influence SAMs growth, such as the PAs concentration in the solution with ethanol, the actual ratio between BPA:Br-BPA, or the immersion time. The variation in V_{oc} and EL emission maximum due to different immersion times for SAMs growth is reported in Figure S4 in the Supporting Information. The linear relation between V_{oc} and the EL emission maximum is preserved in all cases (Figure S4 in the Supporting Information). We also noted that prolonged operation of the SAM-modified hybrid devices lead to an (irreversible) appearance of an EL peak at ca. 1.1 eV, that is, the same position as the EL maximum of the ZnO/ α -NPD device. This suggests that this peak originates from the burn-in of defects in the SAM.

Notably, the shift of both the EL maximum and the V_{oc} by mixing two SAM molecules is gradual and continuous, without

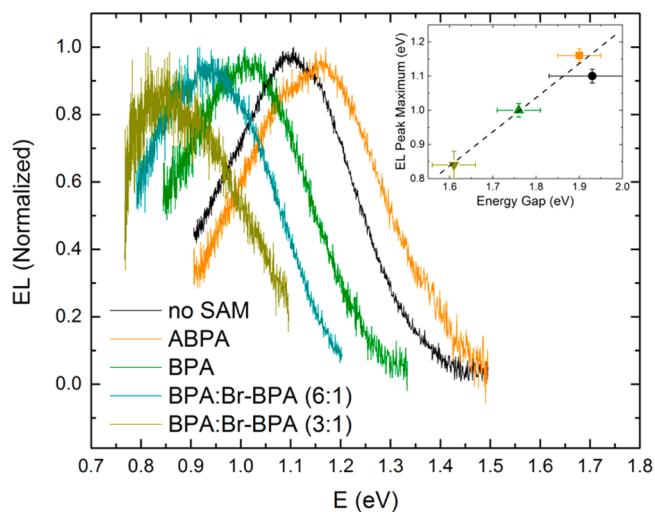


Figure 3. Electroluminescence from α -NPD deposited on SAM-modified ZnO. Increasing the work function of ZnO correlates with a prominent red shift of the EL emission peak (inset).

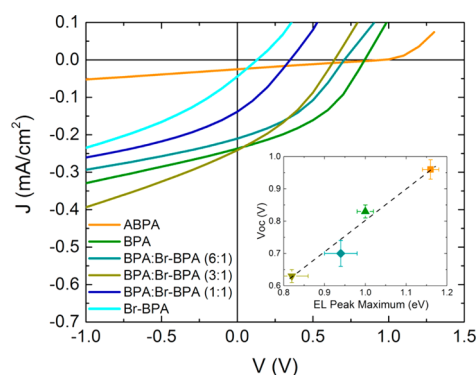


Figure 4. J – V curves of devices using α -NPD as donor and modified ZnO as acceptor. The open-circuit voltage (V_{oc}) decreases with increasing the ZnO work function. The inset shows V_{oc} as a function of the EL emission maximum. Because of the limited wavelength range of our NIR detector, no CT emission was detected for devices with Br-BPA concentrations of 1:1 (with respect to BPA) and above.

considerable broadening of the EL peak. This important result points to a certain degree of delocalization of the HCTS parallel to the hybrid interface, meaning that its energy is determined by a lateral average of the local work function variation of the modified ZnO surface. This finding is at variance with simulation work by Wu et al.,¹⁵ which pointed to a strong localization of the HCTS horizontal and vertical to the hybrid interface. Notably, recent studies of ternary all-organic blends suggested a rather delocalized nature of the CT state,¹⁸ consistent with our findings for HCTS.

In conclusion, we measured CT-dominated EL and a subgap EQE band related to CT absorption for planar hybrid devices composed of ZnO and α -NPD interface. By varying the work function of the ZnO layer through use of self-assembled monolayers, we were able to tune the energy of the charge transfer state, as evidenced by a lowering of the EL emission peak energy. We find a strict correlation between the energy maximum of the CTS emission, the energy gap at the interface, determined by UPS, and the open-circuit voltage obtained in photovoltaic devices. The results of this investigation prove for the first time that for hybrid organic–inorganic interfaces those three quantities are proportional to each other.

EXPERIMENTAL METHODS

The photovoltaic devices used in this work were produced on indium-tin-oxide (ITO)-coated glass substrates (Optrex) precleaned in acetone, detergent, DI water, and isopropanol and dried under a nitrogen flow. Zinc acetate dihydrate and α -NPD were purchased from Sigma-Aldrich. The ZnO layer was prepared by spincoating the zinc acetate dihydrate precursor¹⁹ on the substrate and annealed at 200 °C for 1 h in air; after this step the samples were moved under a nitrogen atmosphere without further air exposure up to the encapsulation of the devices. The SAMs were grown as described elsewhere²⁵ with an immersion time of 2 h in the respective solution of phosphonic acid in dried ethanol under a nitrogen atmosphere. α -NPD was vacuum-deposited in the configuration ITO/ZnO/(SAM)/ α -NPD/MoO₃/Ag. The devices were sealed using a microscope cover glass from Menzel-Gläser together with Hauntsman Araldite 2011. EL, external quantum efficiency, and J – V characteristics were acquired from sealed devices. The EL spectra were acquired with an Andor SR393i-B spectrometer equipped with two iDus detectors: a silicon detector DU420A-BR-DD and an InGaAs DU491A-1.7. The spectral response of the setup was evaluated by means of a calibrated lamp Oriel 63355. For the EQE measurements, light from quartz halogen lamps is coupled into a monochromator, and the intensity is calibrated with a silicon-photodiode and an InGaAs-photodiode. J – V characteristics were measured under AM1.5G condition with a solar simulator from Newport, model 94042A. Samples for photoelectron spectroscopy measurements were transferred into an Omicron Compact-based UHV vacuum system without breaking the protective nitrogen atmosphere. α -NPD was evaporated from resistively heated quartz crucibles. Photoelectrons were excited using a Helium gas discharge lamp HeI_{α} = 21.21 eV for UPS, and for XPS Al K $_{\alpha}$ radiation was used. Electrons were detected by an Omicron EA125 spectrometer with an energy resolution below 120 meV. The samples were biased to –10 V to measure work functions.

ASSOCIATED CONTENT

Supporting Information

More information on the EQE spectra, the PES spectra used to calculate the energy levels at the interface, and the variations of V_{oc} and EL emission maximum when the SAMs are grown with different immersion times. This material is available free of charge via the Internet at <http://pubs.acs.org>.

AUTHOR INFORMATION

Corresponding Authors

*E-mail: fortunato.piersimoni@uni-potsdam.de (F.P.).

*E-mail: koen.vandewal@iapp.de (K.V.).

*E-mail: neher@uni-potsdam.de (D.N.).

Notes

The authors declare no competing financial interest.

ACKNOWLEDGMENTS

We thank Georg Heimel, Sylke Blumstengel, Fritz Henneberger (all HU Berlin), and Wolfgang Brütting (Universität Augsburg) for fruitful discussions and helpful advice. The work was supported by the German Research Foundation (DFG) via the SFB 951 “HIOS” and the SPP 1355, the German Federal Ministry for Education and Research (BMBF) through the InnoProfile project “Organische p-i-n Bauelemente 2.2”, and the Helmholtz-Energie-Allianz “Hybridphotovoltaik”.

REFERENCES

- (1) Benson-Smith, J.; Goris, L.; Vandewal, K.; Haenen, K.; Manca, J.; Vanderzande, D.; Bradley, D.; Nelson, J. Formation of a Ground-State Charge-Transfer Complex in Polyfluorene/[6, 6]-Phenyl-C61 Butyric Acid Methyl Ester (PCBM) Blend Films and Its Role in the Function of Polymer/PCBM Solar Cells. *Adv. Funct. Mater.* **2007**, *17*, 451–457.
- (2) Vandewal, K.; Albrecht, S.; Hoke, E. T.; Graham, K. R.; Widmer, J.; Douglas, J. D.; Schubert, M.; Mateker, W. R.; Bloking, J. T.; Burkhard, G. F.; et al. Efficient Charge Generation by Relaxed Charge-Transfer States at Organic Interfaces. *Nat. Mater.* **2013**, *13*, 63–68.
- (3) Vandewal, K.; Tvingstedt, K.; Gadisa, A.; Inganas, O.; Manca, J. V. On the Origin of the Open-Circuit Voltage of Polymer-Fullerene Solar Cells. *Nat. Mater.* **2009**, *8*, 904–909.
- (4) Faist, M.; Kirchartz, T.; Gong, W.; Ashraf, R.; McCulloch, I.; de Mello, J.; Ekins-Daukes, N.; Bradley, D.; Nelson, J. Competition Between the Charge Transfer State and the Singlet States of Donor or Acceptor Limiting the Efficiency in Polymer: Fullerene Solar Cells. *J. Am. Chem. Soc.* **2012**, *134*, 685–692.
- (5) Dimitrov, S.; Bakulin, A.; Nielsen, C.; Schroeder, B.; Du, J.; Bronstein, H.; McCulloch, I.; Friend, R.; Durrant, J. On the Energetic Dependence of Charge Separation in Low-Band-Gap Polymer/Fullerene Blends. *J. Am. Chem. Soc.* **2012**, *134*, 18189–18192.
- (6) Deibel, C.; Strobel, T.; Dyakonov, V. Role of the Charge Transfer State in Organic Donor–Acceptor Solar Cells. *Adv. Mater.* **2010**, *22*, 4097–4111.
- (7) Bakulin, A. A.; Dimitrov, S. D.; Rao, A.; Chow, P. C.; Nielsen, C. B.; Schroeder, B. C.; McCulloch, I.; Bakker, H. J.; Durrant, J. R.; Friend, R. H. Charge-Transfer State Dynamics Following Hole and Electron Transfer in Organic Photovoltaic Devices. *J. Phys. Chem. Lett.* **2012**, *4*, 209–215.
- (8) Grancini, G.; Maiuri, M.; Fazzi, D.; Petrozza, A.; Egelhaaf, H.-J.; Brida, D.; Cerullo, G.; Lanzani, G. Hot Exciton Dissociation in Polymer Solar Cells. *Nat. Mater.* **2013**, *12*, 29–33.
- (9) Bakulin, A. A.; Rao, A.; Pavelyev, V. G.; Loosdrecht, P. H. M. V.; Pshenichnikov, M. S.; Niedzialek, D.; Cornil, J.; Beljonne, D.; Friend, R. H. The Role of Driving Energy and Delocalized States for Charge Separation in Organic Semiconductors. *Science* **2012**, *335*, 1340–1344.
- (10) Haeldermans, I.; Vandewal, K.; Oosterbaan, W.; Gadisa, A.; D’haen, J.; Van Bael, M.; Manca, J.; Mullens, J. Ground-State Charge-

Transfer Complex Formation in Hybrid Poly (3-Hexyl Thiophene): Titanium Dioxide Solar Cells. *Appl. Phys. Lett.* **2008**, *93*, 223302(1–3).

(11) Bansal, N.; Reynolds, L. X.; MacLachlan, A.; Lutz, T.; Ashraf, R. S.; Zhang, W.; Nielsen, C. B.; McCulloch, I.; Rebois, D. G.; Kirchartz, T.; et al. Influence of Crystallinity and Energetics on Charge Separation in Polymer–Inorganic Nanocomposite Films for Solar Cells. *Sci. Rep.* **2013**, *3*, 1531(1–8).

(12) Renshaw, C. K.; Forrest, S. R. Excited State and Charge Dynamics of Hybrid Organic/Inorganic Heterojunctions. I. Theory. *Phys. Rev. B* **2014**, *90*, 045302(1–15).

(13) Panda, A.; Renshaw, C. K.; Oskooi, A.; Lee, K.; Forrest, S. R. Excited State and Charge Dynamics of Hybrid Organic/Inorganic Heterojunctions. II. Experiment. *Phys. Rev. B* **2014**, *90*, 045303(1–12).

(14) Vaynzof, Y.; Bakulin, A. A.; Gélinas, S.; Friend, R. H. Direct Observation of Photoinduced Bound Charge-Pair States at an Organic-Inorganic Semiconductor Interface. *Phys. Rev. Lett.* **2012**, *108*, 246605(1–5).

(15) Wu, G.; Li, Z.; Zhang, X.; Lu, G. Charge Separation and Exciton Dynamics at Polymer/ZnO Interface From First-Principles Simulations. *J. Phys. Chem. Lett.* **2014**, *5*, 2649–2656.

(16) Chan, M. H.; Chen, J. Y.; Lin, T. Y.; Chen, Y. F. Direct Evidence of Type II Band Alignment in ZnO Nanorods/Poly(3-Hexylthiophene) Heterostructures. *Appl. Phys. Lett.* **2012**, *100*, 021912(1–3).

(17) IUPAC Goldbook Definition of Charge Transfer State. <http://Goldbook.Iupac.org/C01006.html> (accessed January 2015).

(18) Street, R. A.; Davies, D.; Khlyabich, P. P.; Burkhart, B.; Thompson, B. C. Origin of the Tunable Open-Circuit Voltage in Ternary Blend Bulk Heterojunction Organic Solar Cells. *J. Am. Chem. Soc.* **2013**, *135*, 986–989.

(19) Sun, Y.; Seo, J. H.; Takacs, C. J.; Seifert, J.; Heeger, A. J. Inverted Polymer Solar Cells Integrated with a Low-Temperature-Annealed Sol-Gel-Derived ZnO Film as an Electron Transport Layer. *Adv. Mater.* **2011**, *23*, 1679–1683.

(20) Kedem, N.; Blumstengel, S.; Henneberger, F.; Cohen, H.; Hodes, G.; Cahen, D. Morphology-, Synthesis- and Doping-Independent Tuning of ZnO Work Function Using Phenylphosphonates. *Phys. Chem. Chem. Phys.* **2014**, *16*, 8310–8319.

(21) Vandewal, K.; Tvingstedt, K.; Gadisa, A.; Inganäs, O.; Manca, J. Relating the Open-Circuit Voltage to Interface Molecular Properties of Donor: Acceptor Bulk Heterojunction Solar Cells. *Phys. Rev. B* **2010**, *81*, 125204(1–8).

(22) Heimel, G.; Romaner, L.; Zojer, E.; Brédas, J.-L. The Interface Energetics of Self-Assembled Monolayers on Metals. *Acc. Chem. Res.* **2008**, *41*, 721–729.

(23) Hotchkiss, P. J.; Li, H.; Paramonov, P. B.; Paniagua, S. A.; Jones, S. C.; Armstrong, N. R.; Brédas, J.-L.; Marder, S. R. Modification of the Surface Properties of Indium Tin Oxide with Benzylphosphonic Acids: a Joint Experimental and Theoretical Study. *Adv. Mater.* **2009**, *21*, 4496–4501.

(24) Wood, C.; Li, H.; Winget, P.; Brédas, J.-L. Binding Modes of Fluorinated Benzylphosphonic Acids on the Polar ZnO Surface and Impact on Work Function. *J. Phys. Chem. C* **2012**, *116*, 19125–19133.

(25) Lange, I.; Reiter, S.; Pätzelt, M.; Zykov, A.; Nefedov, A.; Hildebrandt, J.; Hecht, S.; Kowarik, S.; Wöll, C.; Heimel, G.; et al. Tuning the Work Function of Polar Zinc Oxide Surfaces Using Modified Phosphonic Acid Self-Assembled Monolayers. *Adv. Funct. Mater.* **2014**, *24*, 7014–7024.

(26) Schlesinger, R.; Xu, Y.; Hofmann, O. T.; Winkler, S.; Frisch, J.; Niederhausen, J.; Vollmer, A.; Blumstengel, S.; Henneberger, F.; Rinke, P.; et al. Controlling the Work Function of ZnO and the Energy-Level Alignment at the Interface to Organic Semiconductors with a Molecular Electron Acceptor. *Phys. Rev. B* **2013**, *87*, 155311.

(27) Graham, K. R.; Erwin, P.; Nordlund, D.; Vandewal, K.; Li, R.; Ngongang Ndjawa, G. O.; Hoke, E. T.; Salleo, A.; Thompson, M. E.; McGehee, M. D.; et al. Re-Evaluating the Role of Sterics and Electronic Coupling in Determining the Open-Circuit Voltage of Organic Solar Cells. *Adv. Mater.* **2013**, *25*, 6076–6082.